NATIONAL ADVISORY COMMITTEE FOR AERONAUTICS

TECHNICAL NOTE

No. 1889

BIAXIAL FATIGUE STRENGTH OF 24S-T ALUMINUM ALLOY

By Joseph Marin and William Shelson

The Pennsylvania State College

Washington
May 1949

NATIONAL ADVISORY COMMITTEE FOR AERONAUTICS

TECHNICAL NOTE NO. 1889

BIAXIAL FATIGUE STRENGTH OF 24S-T ALUMINUM ALLOY[1]

By Joseph Marin and William Shelson

SUMMARY

The object of this investigation was to determine the fatigue-strength values for 24S-T aluminum alloy when subjected to various ratios of biaxial stresses. The biaxial stresses considered were both tensile. The influence of various ratios of the maximum values of the principal stresses upon the fatigue strength was determined. Fluctuating biaxial tensile stresses were produced by applying a pulsating internal pressure and an axial tensile load to a thin-walled tubular specimen. The maximum and minimum values of the principal stresses were kept in phase. To apply the dynamic loads, a new type of testing machine was designed and constructed.

S-N diagrams for four principal stress ratios were obtained for defining the fatigue strength up to 5×10^6 cycles. An attempt was made to compare the test results with a modified maximum-stress theory of failure but poor agreement was found between theory and test results. The test results show that the uniaxial fatigue strength in the transverse direction of the tubular specimens may be about 60 percent of the fatigue strength in the longitudinal direction.

INTRODUCTION

Many machine and structural parts are subjected to stresses that vary in magnitude with time. For example, a connecting rod may be subjected to fluctuating axial stress which varies from a minimum value σ_{min} to a maximum value σ_{max}, as shown in figure 1. The stress variation in figure 1 can be considered to be made up of a completely reversed or variable stress σ_r superimposed upon a steady mean stress σ_m. To determine strength of materials under fluctuating or fatigue stresses, a series of tests are made in a fatigue testing machine. In these tests the specimens are subjected to a given mean stress σ_m and to different values of the maximum stress. For each test the number of cycles of stress required to produce rupture of the specimen are determined and a σ_{max}-N diagram is plotted as shown in figure 2. For a fixed mean stress it is apparent, as shown in figure 2, that the lower the maximum stress

[1]New temper designation for alloy used: 24S-T4.

the greater will be the number of stress cycles that can be applied before failure occurs. The value of the maximum stress for a given number of stress cycles, as obtained from the experimental data such as figure 2, is called "the fatigue strength" of the material. The fatigue strength will depend not only upon the number of cycles of stress but also upon the value of the mean stress.

Most fatigue tests are made on specimens subjected to simple stresses, including fluctuating axial stresses, as described in the foregoing paragraph, or fluctuating bending stresses. In machine and structural parts, however, the fluctuating stresses are often not simple or uniaxial stresses, but may be biaxial or triaxial and act in more than one direction. There is very little information on the fatigue strength of metals subjected to combined stresses. A survey of most of the available data is given in reference 1. The purpose of this investigation was to obtain the fatigue strength of 24S-T aluminum alloy when subjected to various ratios of biaxial fatigue stresses. Fluctuating biaxial tensile stresses were produced by subjecting a tubular specimen to fluctuating axial tension and fluctuating internal pressure.

The project was conducted by the School of Engineering of The Pennsylvania State College under the sponsorship and with the financial assistance of the National Advisory Committee for Aeronautics. The tests were conducted in the Combined Stress Laboratory of the Department of Engineering Mechanics. Professor K. J. DeJuhasz of the Engineering Experiment Station gave valuable suggestions on the design of the testing machine. The testing machine was built by Messrs. M. Aikey, H. Johnson, and S. S. Eckley. Messrs. William Shelson and V. L. Dutton, research assistants, conducted the tests and computed the test data. The administrative direction given by the NACA and the College of Engineering and the technical assistance given by the foregoing individuals is greatly appreciated. The testing machine was designed by Joseph Marin, who directed the project and prepared this report.

SYMBOLS

A	cross-sectional area of tubular specimen, square inches
d	internal diameter of specimen, inches
N	number of stress cycles to failure
p	internal pressure, psi
P	axial tensile load, pounds
p', p'', p'''	maximum, mean, and minimum fluctuating pressure, respectively, psi

P', P'', P'''	maximum, mean, and minimum fluctuating axial tension loads, respectively, pounds
R	principal stress ratio $\left(\sigma_2/\sigma_1 = \sigma_2'/\sigma_1' = \sigma_2''/\sigma_1''\right)$
σ	uniaxial tensile stress, psi
σ_{max}, σ_m, σ_{min}, σ_r	maximum, mean, minimum, and variable uniaxial tensile stresses, psi
σ_1, σ_2	longitudinal and transverse biaxial principal stresses, psi
σ_1', σ_1'', σ_1'''	maximum, mean, and minimum values of principal stress σ_1, respectively, psi
σ_2', σ_2'', σ_2'''	maximum, mean, and minimum values of principal stress σ_2, respectively, psi
σ_{1t}'	fatigue strength for uniaxial longitudinal tension, psi
σ_{1y}, σ_{2y}	biaxial yield-strength values, psi
σ_{1u}, σ_{2u}	biaxial nominal ultimate-strength values, psi

DESCRIPTION OF MATERIAL

The material tested in this investigation was a fully heat-treated aluminum alloy designated as 24S-T. The material was received in tubular extruded form in lengths of 16 feet, with an internal diameter of 2 inches and a wall thickness of 1/4 inch. The nominal chemical composition, in addition to aluminum and normal impurities, consists of 4.4 percent copper, 1.5 percent magnesium, and 0.6 percent manganese. The mechanical properties, as furnished by the manufacturer, are: Tensile strength = 68,000 psi; yield strength (0.2-percent offset) = 44,000 psi; modulus of elasticity = 10.6×10^6 psi; percentage elongation (in 2 in.) = 14 percent; and Poisson's ratio = 0.33.

Tensile control tests were made on flat specimens machined from the walls of the tubular extrusions. The results of these tests are reported in reference 2.

TEST PROCEDURE

Test Specimen

The fatigue test specimens were machined from tubular sections about $16\frac{1}{2}$ inches long, with an inside diameter of 2 inches and a wall thickness of $\frac{1}{4}$ inch. The finished specimen is shown in figure 3 and has an over-all length of 16 inches. The other dimensions of the specimen are shown in figure 3. The inner walls of the specimens were left in the as-extruded form while the outer surfaces were polished circumferentially to a 9/0 finish with metallurgical abrasive paper. The wall thickness was measured to 0.0001 inch by a special apparatus as described in reference 2. The wall-thickness values were measured at five equal intervals along the tube length and six readings were taken around the circumference at each interval. The outside diameters at each interval in two perpendicular directions were also measured. The ratio of wall thickness to diameter of the specimen was 0.025, so that the stresses throughout the wall were essentially uniform. The circumferential elastic stress produced by internal pressure, as calculated assuming a thin wall and uniform stress distribution, is about 3 percent less than the exact value, while the axial stress, calculated assuming a thin wall, is about 2 percent more than the exact value. The ratio of diameter to reduced length of the specimen is about 0.25, thereby providing a sufficiently long section of the specimen free from the bending stresses produced by end restraints.

For a thin-walled tubular specimen subjected to an axial tensile load P and an internal pressure of p psi, the longitudinal and circumferential stresses are, respectively,

$$\sigma_1 = \frac{P}{A} + \frac{pd}{4t} = \frac{P}{\pi dt} + \frac{pd}{4t} \tag{1}$$

$$\sigma_2 = \frac{pd}{2t} \tag{2}$$

where

A	cross-sectional area of tube
d	internal diameter of specimen
t	tube-wall thickness

The tubular specimens are subjected to synchronous variable loads P and p which have maximum values P' and p', minimum values P''' and p''', and mean values P'' and p''. The maximum, minimum, and mean values of the principal stresses σ_1 and σ_2 are

$$\left.\begin{aligned} \sigma_1' &= \frac{P'}{\pi dt} + \frac{p'd}{4t} \\ \sigma_1''' &= \frac{P'''}{\pi dt} + \frac{p'''d}{4t} \\ \sigma_1'' &= \frac{P''}{\pi dt} + \frac{p''d}{4t} \end{aligned}\right\} \tag{3}$$

$$\left.\begin{aligned} \sigma_2' &= \frac{p'd}{2t} \\ \sigma_2''' &= \frac{p'''d}{2t} \\ \sigma_2'' &= \frac{p''d}{2t} \end{aligned}\right\} \tag{4}$$

The fatigue strength of a material when subjected to the stresses in equations (3) and (4) depends upon both the ratio of the minimum to maximum stresses and to the ratio of the principal stresses. Since a very large number of tests would be required to cover completely all possible stress combinations, it was necessary to restrict the test program to a consideration of the influence of the principal stress ratio σ_2'/σ_1' only.

In this investigation the ratios of minimum to maximum stresses σ_1'''/σ_1' and σ_2'''/σ_2' varied from about 0.10 to 0.20.

Testing Machine

A special testing machine was designed and built for applying the fluctuating internal pressures and axial loads referred to in the foregoing section. Figures 4 and 5 show schematic drawings of the testing machine, while figure 6 is a photograph of the complete machine. Figures 7 to 11 are close-up photographs of various parts showing details of construction and operation of the machine.

The tubular specimen S is subjected to an axial fluctuating load by the lever K (fig. 6). This lever is subjected to a fluctuating

load by means of an eccentric E_1. The eccentric E_1 is attached to a gear G_2 which is driven by a pinion G_1 and operated by a 3-horsepower, 3600-rpm, alternating-current motor T (fig. 7). A gear reduction of 1 to 10 produces about 300 fluctuations of stress per minute at the specimen. This low rate of stress fluctuation was necessary to eliminate possible errors due to interference of pressure waves produced by the successive application of internal pressure.

The internal oil pressure is applied to the specimen by means of the piston in a Bosch pump I. The pump I is actuated by a plunger and connecting-rod system attached to a driving eccentric E_2 (fig. 8). The eccentric E_2 is adjustable with respect to throw and phase angle between the two eccentrics E_1 and E_2 which are mounted on the same shaft. The pressure obtained in the specimen S is raised by increasing the throw of the eccentric and, consequently, the stroke of the piston. A steel cylindrical plug, with dimensions slightly less than the inner dimensions of the specimen, is inserted in the specimen to reduce the total volume of fluid in the pressure system and so permit higher pressure. To provide against drop in pressure caused by possible oil leakage, an accumulator A with a check valve C (fig. 10) is connected to the specimen. The accumulator A is a standard aircraft-type accumulator in which air is used as the pressure-maintaining medium.

A revolution counter U is used to record the number of stress fluctuations to fracture. The motor is stopped by a microswitch when the specimen is fractured. For axial tension without internal pressure a microswitch is mounted on the lever K so that, when the specimen fractures, the yoke Y below the specimen rotates and operates the microswitch which stops the motor. For tests in which internal pressure is used, fracture of the specimen causes a drop in pressure, which releases the plunger in the valve P. This operates the microswitch M which in turn stops the motor.

The axial load is measured by a 10,000-pound dynamometer N (fig. 9) which transmits the load from the eccentric E_1 to the lever. A threaded turn-buckle unit between the eccentric and the dynamometer allows the adjustment of the minimum axial load. The lever with a 4-to-1 ratio applies the load to the specimen. The specimen is held between two spherical seats to insure axiality of loading.

The maximum and minimum pressures are measured by Bourdon gages H and L, respectively. The gages are connected to the piping with specially designed check valves so that the pointers of the gages do not fluctuate, but move only if there is a change in the values of the maximum or minimum pressures. In this way the gage mechanisms are not subjected to fluctuating stresses.

Calibration of Testing Machines

The lever K for applying the load was calibrated by noting simultaneous dial readings on a 10,000-pound dynamometer N and strain readings of a calibrated test bar inserted in place of the specimen S. The test bar was calibrated in a Baldwin-Southwark hydraulic testing machine. The strains of the steel test bar were measured by two SR-4 electric strain gages cemented to opposite sides of the bar.

Concentricity of the axial tensile loading on the specimen was checked by measuring the elongation of the specimen at four locations equally spaced around the circumference. After adjustment of the holders, the strains were found to be in reasonable agreement for loads within the range of the tests. The maximum difference in the measured stress on opposite sides of the specimen was less than 1 percent.

Calculations were also made to determine the error introduced in the axial-load values by neglecting the axial load produced by the inertia forces in the lever. These inertia forces were produced by the accelerations in the lever as the fluctuating axial load was applied. Calculation shows that the maximum error is less than 1 percent of the applied load.

The pressure gages were calibrated with a dead-weight gage tester. The maximum-pressure gage has a range of 0 to 5000 psi and the minimum-pressure gage a range of 0 to 2000 psi. Readings of the pressure were noted to the nearest 25 psi.

Method of Testing

The test procedure outlined in the following paragraphs applies to tests in which the specimen was subjected to both an axial load and internal pressure. For tests in which only axial load or internal pressure was used the procedure was simplified by the omission of some of the adjustments.

After the dimensions of a specimen are measured, as explained in reference 2, the specimen is screwed into the specimen holders. The axial load is adjusted as follows: The axial load, corresponding to a given value, can be applied by adjusting the eccentric E_1 to a given position and fixing that position with self-locking set screws. With the eccentric E_1 (fig. 7) in its lowest position, a threaded turnbuckle above the dynamometer N is adjusted until the dynamometer registers the minimum load desired. The eccentric drive shaft is next rotated by hand to determine the maximum axial-load reading on the dynamometer. If this reading has changed, the above procedure is repeated until the correct minimum and maximum axial-load readings are registered on the dynamometer.

Before making the internal-pressure adjustments, the oil-pressure line is first fastened to the connection in the lower specimen holder. Various values of maximum- and minimum-pressure readings can be obtained by varying the setting of the eccentric E_2 (fig. 8). To apply selected values of the maximum and minimum pressure, a tentative setting of the outer part of the eccentric to the inner part is first made. By means of the hand pump B, the internal-pressure system is filled with oil and the air outlet at the top of the specimen is closed when all the air is expelled from the system. Operation of the hand pump is then continued until the desired minimum internal pressure is reached with the piston of the Bosch pump at the bottom of its stroke. The eccentric drive shaft is now rotated by hand to obtain approximate readings of the minimum and maximum pressures. If the pressure readings are close to the values desired, the motor is switched on so that the actual pressures may be noted. The pressures under dynamic loading with the motor operating are slightly higher than under static loading produced when the shaft is turned by hand. The valve F in the pressure line leading to the pressure gages (fig. 10) is closed during the starting period to avoid shock loading. During a test, however, the valve F is open. Fluctuations of the gages are prevented by a specially designed valve block G, which permits static readings of the maximum pressure on gage H and the minimum pressure on gage L.

The phase angle between the axial tensile load and the internal pressure can be varied by rotating the inner part of the eccentric E_2 relative to the inner part of eccentric E_1. To obtain synchronism of the two loads, the eccentrics are adjusted so that the minimum dynamometer axial-load reading is obtained when the piston of the Bosch pump is at the bottom of its stroke.

After the desired internal-pressure values are obtained, the axial loading is checked, since the elongation of the specimen produced by the internal pressure reduces slightly the external load produced by the lever. If necessary, the eccentrics E_1 and then E_2 are again adjusted to give the required values of pressure and axial loads. After the machine has been in operation for about an hour, load adjustments may again be necessary because of changes in temperature of the oil or loosening of the mechanical linkage. To insure correct loading during a test, the loads are checked several times a day. Occasionally it is necessary to add more oil to the system to replace leakage. This is done by means of the hand pump. When the specimen fails, one of the microswitches shuts off the motor, and a record of the number of cycles to failure is recorded by the counter U.

TEST RESULTS

The fatigue strengths were obtained in this investigation for four principal stress ratios and for ratios of minimum to maximum stress

equal to approximately zero. Strengths were determined for various numbers of stress application up to about 2×10^6 cycles. The S–N or σ–N diagrams for the four principal stress ratios are shown in figure 12. The data used in plotting the diagrams in figure 13 are shown in tables 1 to 4. Since it was necessary to limit the stress applications to a low rate to avoid interference of pressure waves, the tests had to be limited to a relatively low number of stress cycles, as shown in figure 13.

ANALYSIS AND DISCUSSION

The influence of the principal stress ratio on the fatigue strength is shown in figure 14, which shows in a single plot the curves from the S–N diagrams of figure 12. The influence of the principal stress ratio on the fatigue strength can be shown more clearly than in figure 12 by a comparison of the biaxial fatigue strengths (σ_1' or σ_2') with the longitudinal uniaxial fatigue strengths σ_{1t}'. The strength ratios for various numbers of cycles as shown in figure 13 are in terms of coordinates σ_1'/σ_{1t}' and σ_2'/σ_{1t}', where σ_{1t}' is the fatigue strength for uniaxial longitudinal tension for a given value of N and σ_1' and σ_2' are the principal stress values for the same value of N.

Attempts were made to compare the test results in figure 15 with the theories of failure (reference 2), but no existing theory was found adequate. That is, all the theories require that the material be homogeneous and isotropic, so that the uniaxial strengths σ_{1t}' and σ_{2t}' in the longitudinal and circumferential directions are equal according to these theories. An examination of figure 13 shows that this is far from being true. Figure 13 indicates that the uniaxial fatigue strengths in the circumferential direction may be about 60 percent of the uniaxial fatigue strengths in the longitudinal direction. That is, the extruded tubular specimens have directional properties with a greater strength in the longitudinal direction. This directional effect was also found for the yield and ultimate static strengths in reference 1 where the yield strength in the circumferential direction was about 90 percent of that in the longitudinal direction and the corresponding percentage for nominal ultimate strength was about 80 percent.

To determine whether a modified maximum-stress theory could be used to interpret the foregoing test results if the directional properties of the material were considered, the fatigue-strength data from this report and the static-strength data from reference 2 were plotted as shown in figures 15 and 16. In plotting figure 16, σ_{1y} and σ_{2y} represent the biaxial yield strengths, and in figure 15, σ_{1u} and σ_{2u} represent the

biaxial nominal ultimate strengths. If a modified maximum-stress theory is to agree with the test results in figure 16, the ratios σ_1'/σ_{1y} and σ_2'/σ_{2y} should remain constant for all values of the principal stress ratio and for each value of N. Figure 16 shows that the stress ratios σ_1'/σ_{1y} and σ_2'/σ_{2y} are not constant. Figure 15 shows that there is also a variation in the strength ratios σ_1'/σ_{1u} and σ_2'/σ_{2u} with variation in the principal stress ratio. That is, a modified maximum-stress theory based on either yield or ultimate strengths does not agree with the test results. However, figures 15 and 16 are of value in showing the relation between the fatigue and static strengths of the material for various ratios of the principal stresses.

In figure 17 a comparison is made between the S-N diagram based on the longitudinal fatigue-stress results reported in the foregoing paragraphs for $\sigma_2/\sigma_1 = 0$ and the S-N diagram based on data given in reference 3 for 0.2-inch-diameter specimens. Figure 17 shows that there is an appreciable reduction in fatigue strengths for the tubular specimens, since the S-N curve for these specimens lies well below that for the solid specimens.

Figure 18 is a photograph of typical fractured specimens. For stress ratios of $\sigma_2/\sigma_1 = 0.5$, the specimens fractured circumferentially. The plane of the fracture was at an angle of about 45° to the surface of the tube. For stress ratios $\sigma_2/\sigma_1 = 1.0$ and $\sigma_2/\sigma_1 = 2.0$, failure was produced by small cracks in the longitudinal direction about 1/2 to 1 inch in length.

CONCLUSIONS

Biaxial tensile fatigue strengths of 24S-T aluminum-alloy tubing were obtained for various ratios of the biaxial maximum stresses and with the minimum stresses approximately equal to zero. The test results show that uniaxial fatigue-strength values in the longitudinal direction cannot be used to predict the fatigue strength, and that the biaxial fatigue strength may be as low as 50 percent of the uniaxial fatigue strength.

The Pennsylvania State College
State College, Pa., December 13, 1947

REFERENCES

1. Marin, Joseph: Interpretation of Experiments on Fatigue Strength of Metals Subjected to Combined Stresses. The Welding Jour., vol. VII, no. 5, May 1942, pp. 245-s – 248-s. (See also, Marin, J.: Mechanical Properties of Materials and Design. McGraw-Hill Book Co., Inc., 1942, ch. 4.)

2. Marin, Joseph, Faupel, J. H., Dutton, V. L., and Brossman, M. W.: Biaxial Plastic Stress-Strain Relations for 24S-T Aluminum Alloy. NACA TN No. 1536, 1948.

3. Anon: Alcoa Structural Handbook. ALCOA, 1945.

TABLE 1.- FATIGUE TEST DATA FOR STRESS RATIO $R = \sigma_2/\sigma_1 = 0$

Specimen	Load, P' (lb)	Load, P''' (lb)	Diameter, d (in.)	Average wall thickness, t (in.)	Stress, σ_1' (psi)	Stress, σ_2' (psi)	Stress, σ_1''' (psi)	Stress, σ_2''' (psi)	Stress ratio, R σ_2'/σ_1'	Number of cycles, N
G-4	16.0×10^3	1.00×10^3	2.00	0.0534	48.0×10^3	0×10^3	3.0×10^3	0×10^3	0	0.0599×10^6
G-3	15.0	1.50	2.00	.0551	13.0	0	4.0	0	0	.0653
F-3	22.0	1.50	2.00	.0766	46.0	0	3.0	0	0	.0733
G-8	11.0	1.00	2.00	.0530	33.0	0	3.0	0	0	.0889
G-7	21.0	1.50	2.00	.0776	43.0	0	3.0	0	0	.0950
G-5	14.5	2.00	2.00	.0530	44.0	0	6.0	0	0	.1070
G-6	11.0	.75	2.00	.0526	33.0	0	2.0	0	0	.1342
H-2	9.5	1.00	2.00	.0527	29.0	0	3.0	0	0	.3105
H-7	7.2	.70	2.00	.0499	23.0	0	2.0	0	0	2.0654

TABLE 2.- FATIGUE TEST DATA FOR STRESS RATIO $R = \sigma_2/\sigma_1 = 2.0$

Specimen	Pressure, p' (psi)	Pressure, p''' (psi)	Diameter, d (in.)	Average wall thickness, t (in.)	Stress, σ_1' (psi)	Stress, σ_2' (psi)	Stress, σ_1''' (psi)	Stress, σ_2''' (psi)	Stress ratio, R σ_2'/σ_1'	Number of cycles, N
H-3	1.750×10^3	0.200×10^3	2.00	0.0507	17.25×10^3	34.50×10^3	2.00×10^3	4.00×10^3	2.0	0.0438×10^6
H-5	1.400	.200	2.00	.0514	13.50	27.00	2.00	4.00	2.0	.0513
H-4	1.400	.200	2.00	.0526	13.25	26.50	2.00	4.00	2.0	.1074
H-6	1.050	.200	2.00	.0533	9.75	19.50	2.00	4.00	2.0	.2185
F-1	.750	.200	2.00	.0471	8.00	16.00	2.00	4.00	2.0	.2395
H-8	.750	.100	2.00	.0525	7.15	14.30	.95	1.90	2.0	.2481
H-5	.750	.125	2.00	.0505	7.41	14.82	1.24	2.48	2.0	.5194
H-10	.825	.200	2.00	.0533	7.75	15.50	2.00	4.00	2.0	.5643
G-10	.625	.125	2.00	.0515	6.06	12.12	1.21	2.42	2.0	8.2253

TABLE 3.- FATIGUE TEST DATA FOR STRESS RATIO $R = \sigma_2/\sigma_1 = 1.0$

Specimen	Load, P' (lb)	Load, P''' (lb)	Pressure, p' (psi)	Pressure, p''' (psi)	Diameter, d (in.)	Average wall thickness, t (in.)	Stress, σ_1' (psi)	Stress, σ_2' (psi)	Stress, σ_1''' (psi)	Stress, σ_2''' (psi)	Stress ratio, R σ_2'/σ_1'	Number of cycles, N
H-10	4.00×10^3	0.50×10^3	1.200×10^3	0.200×10^3	2.00	0.0539	23.0×10^3	22.5×10^3	3.5×10^3	3.5×10^3	0.98	0.0966×10^6
H-8	2.75	.50	.800	.100	2.00	.0540	15.5	15.0	2.5	2.0	.97	.1049
H-5	3.50	1.00	1.050	.200	2.00	.0545	20.0	19.5	4.5	3.5	.98	.1609
H-9	2.50	.50	.750	.100	2.00	.0497	15.5	15.0	2.5	2.0	.97	.1916
H-6	2.50	.50	.800	.125	2.00	.0534	15.0	15.0	2.5	2.5	1.00	.2158
H-4	2.30	.50	.650	.100	2.00	.0545	12.5	12.0	2.5	2.0	.96	1.8679
H-6	1.60	.60	.575	.125	2.00	.0505	10.8	11.4	3.1	2.5	1.06	5.1044
H-7	2.40	1.58	.750	.150	2.00	.0518	14.6	14.5	3.0	2.9	.99	5.1362

TABLE 4.- FATIGUE TEST DATA FOR STRESS RATIO $R = \sigma_2/\sigma_1 = 0.5$

Specimen	Load, P' (lb)	Load, P''' (lb)	Pressure, p' (psi)	Pressure, p''' (psi)	Diameter, d (in.)	Average wall thickness, t (in.)	Stress, σ_1' (psi)	Stress, σ_2' (psi)	Stress, σ_1''' (psi)	Stress, σ_2''' (psi)	Stress ratio, R σ_2'/σ_1'	Number of cycles, N
F-11	7.75×10^3	0.75×10^3	0.850×10^3	0.200×10^3	2.00	0.0543	30.50×10^3	15.50×10^3	4.00×10^3	3.50×10^3	0.51	0.1185×10^6
F-2	8.00	.75	.825	.200	2.00	.0534	32.50	15.50	4.00	3.50	.48	.1320
H-10	10.60	1.00	1.000	.125	2.00	.0545	40.12	18.35	4.07	2.30	.46	.1403
H-11	9.50	.90	.975	.200	2.00	.0527	38.00	18.50	4.50	4.00	.49	.1596
F-3	6.50	1.10	.710	.125	2.00	.0523	26.56	13.58	4.44	2.20	.51	.2450
F-7	4.40	.75	.480	.150	2.00	.0539	17.44	8.91	3.60	2.78	.51	.2600
G-9	5.50	1.10	.600	.125	2.00	.0542	21.66	11.07	4.38	2.30	.51	.5895
H-1	4.10	.50	.425	.125	2.00	.0513	16.86	8.29	2.77	2.44	.49	5.1953

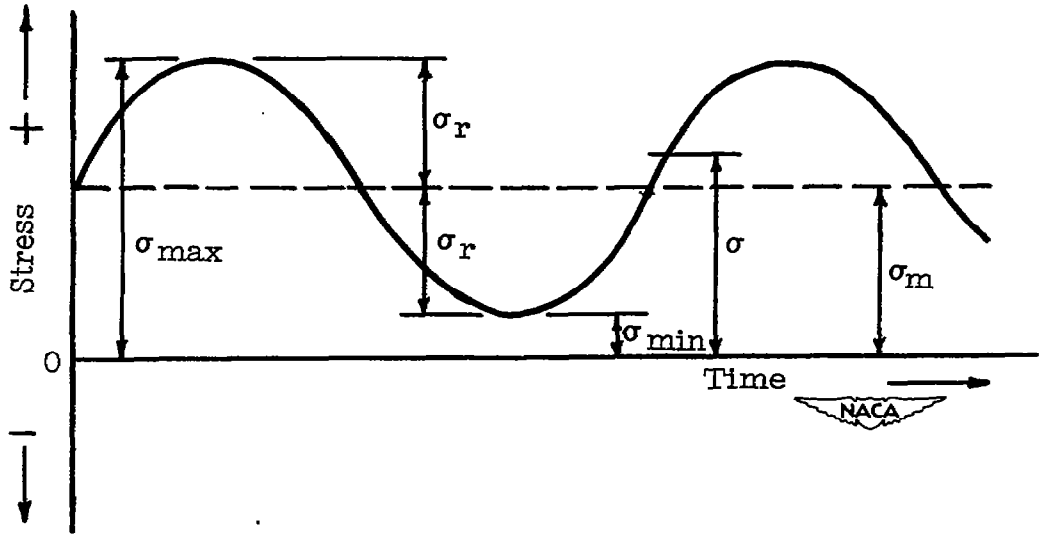

Figure 1.- Nomenclature for fluctuating stresses.

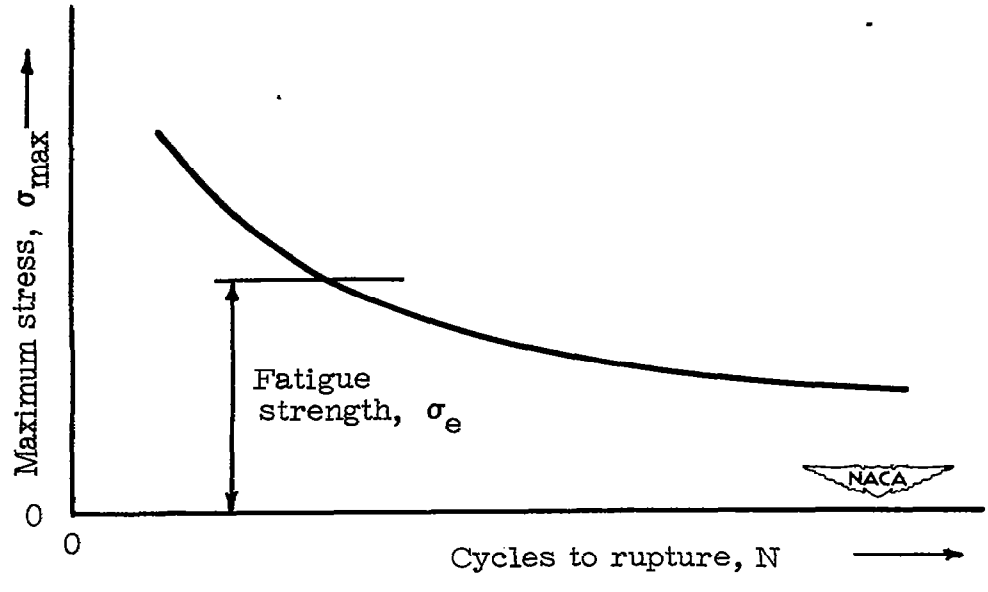

Figure 2.- Typical S-N diagram.

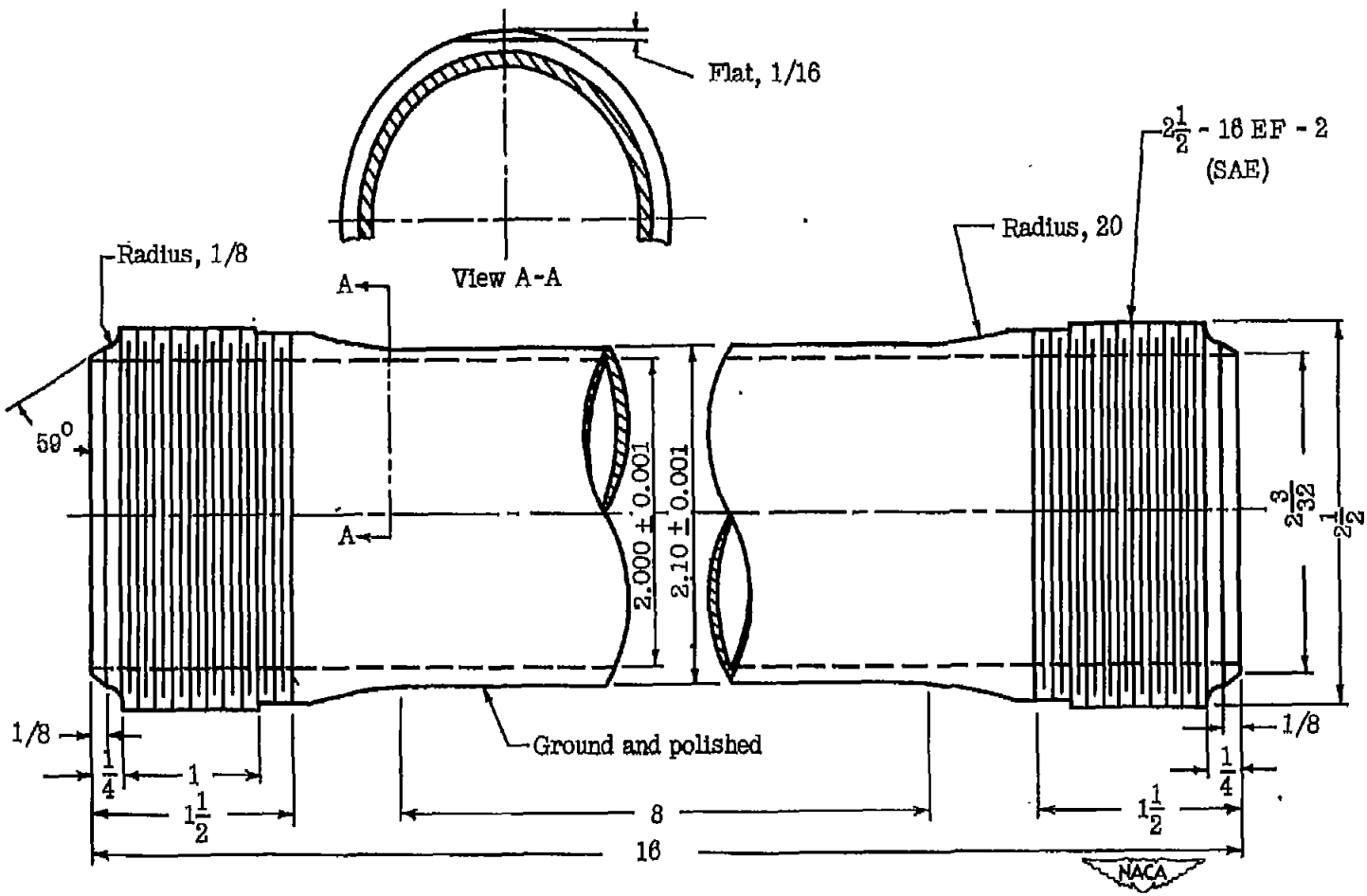

Figure 3.- Biaxial stress specimen. All dimensions are in inches.

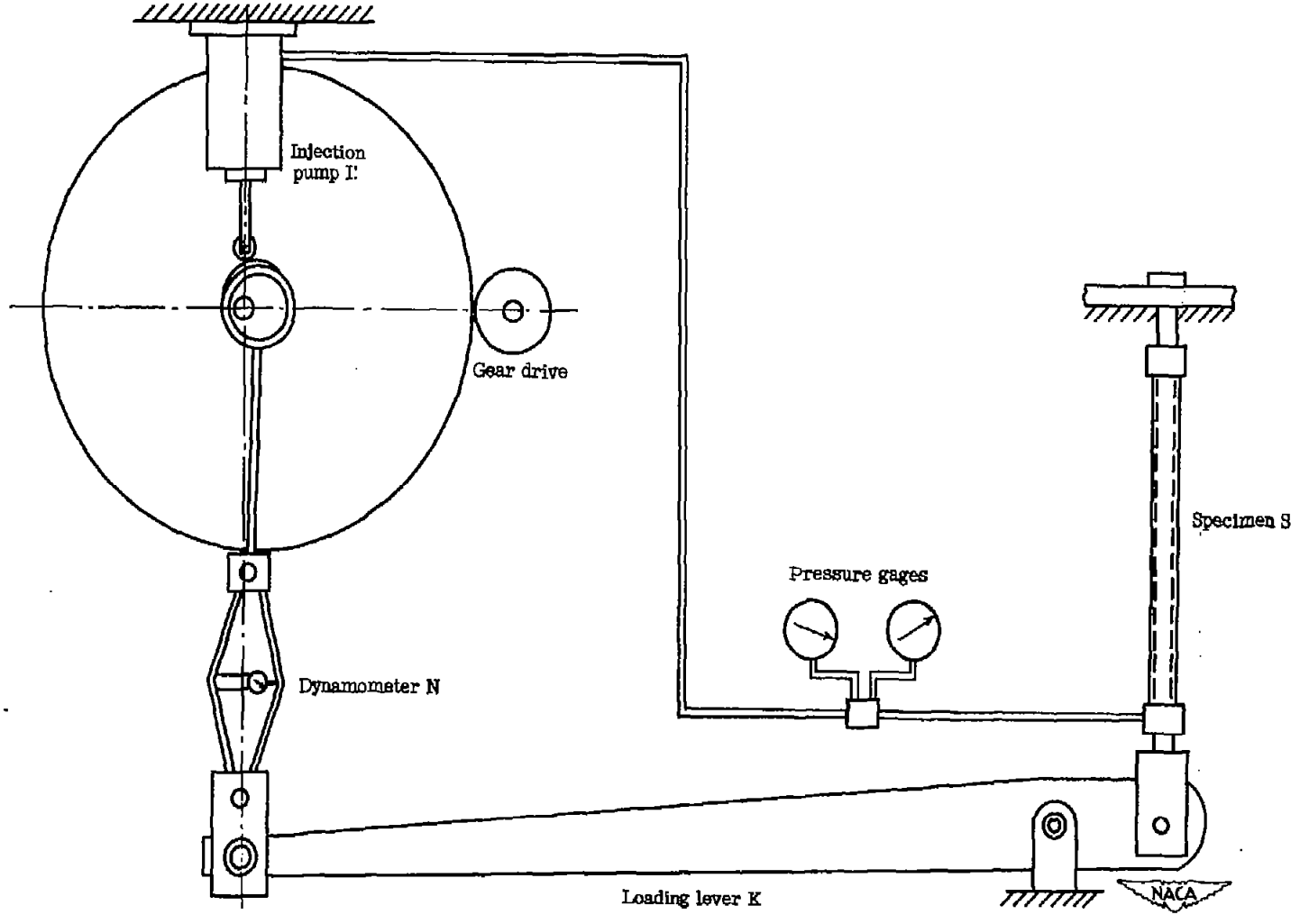

Figure 4.- Axial loading arrangement.

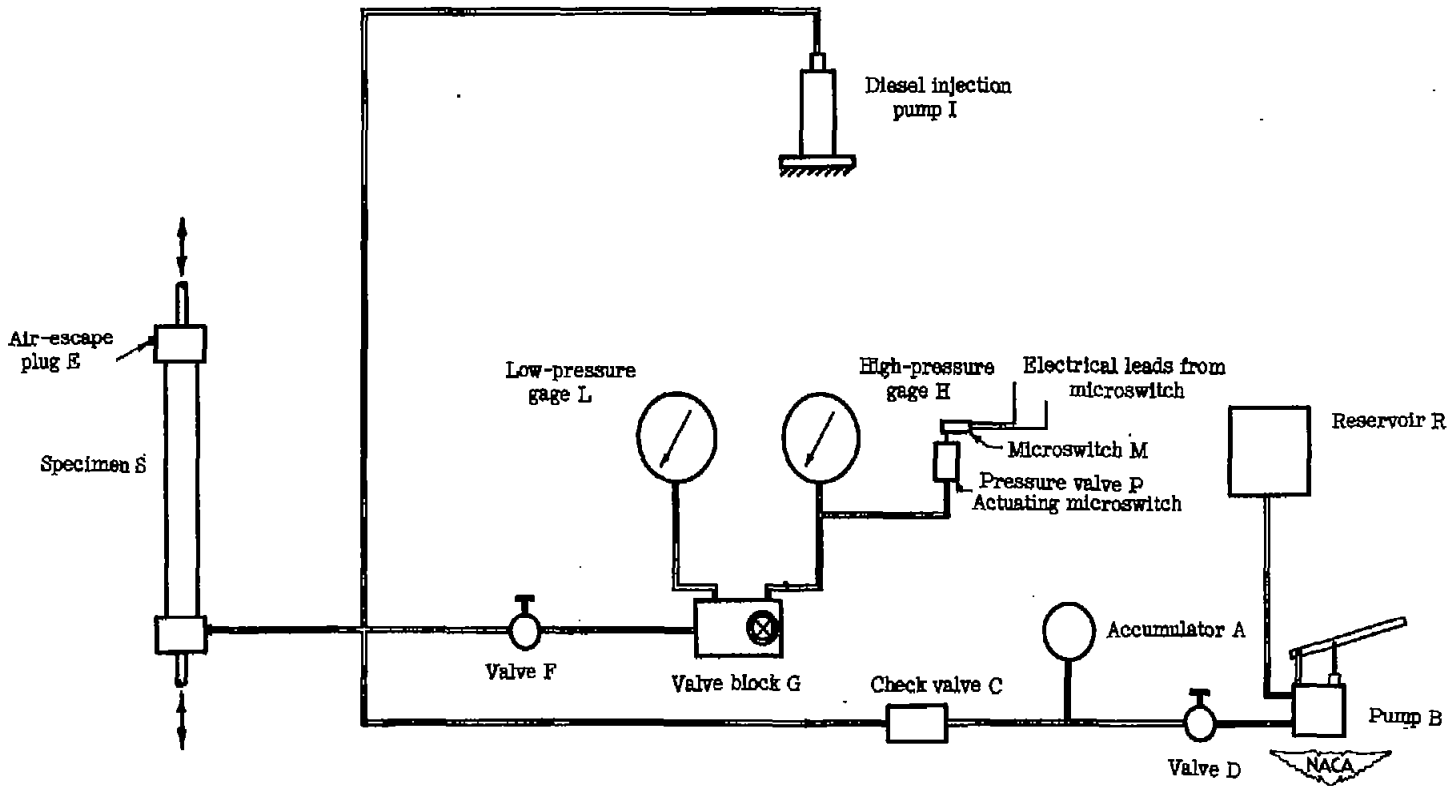

Figure 5.- Internal-pressure loading arrangement.

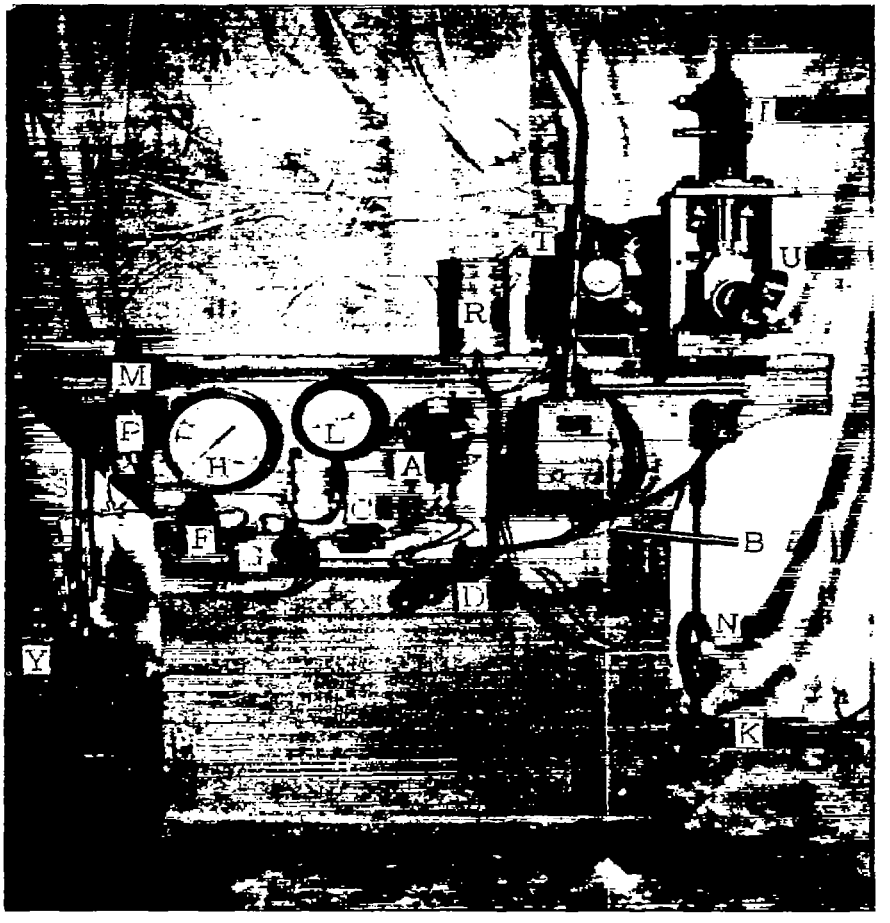

Figure 6.- Biaxial fatigue testing machine.

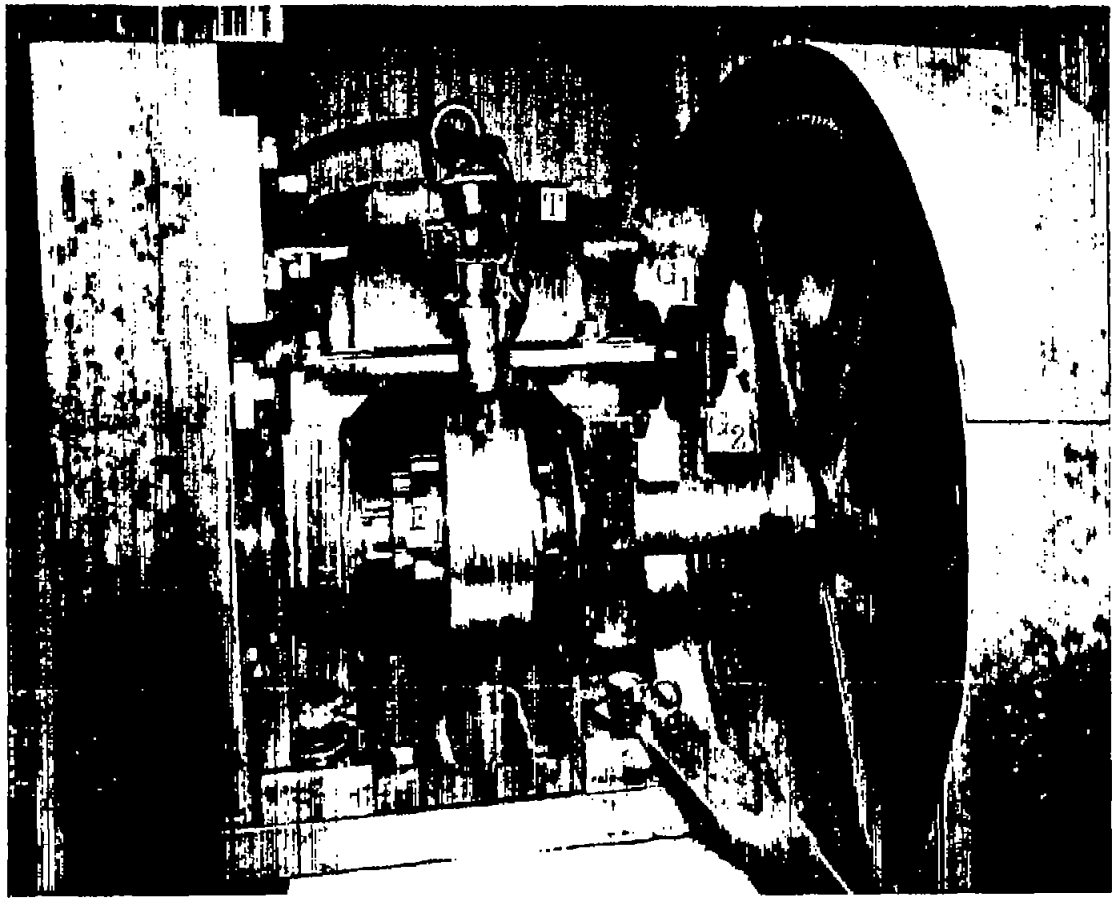

Figure 7.- Drive unit and eccentric.

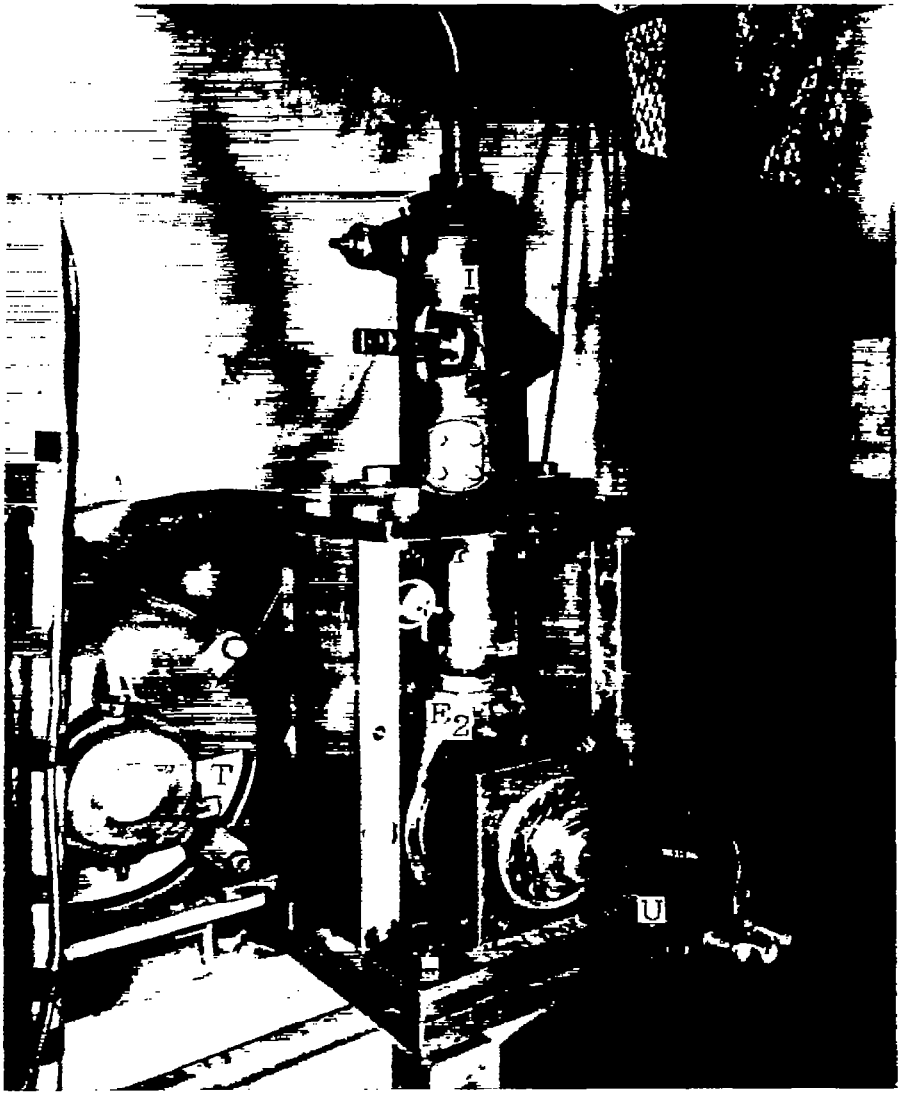

Figure 8.- Bosch pump unit for fluctuating internal pressures.

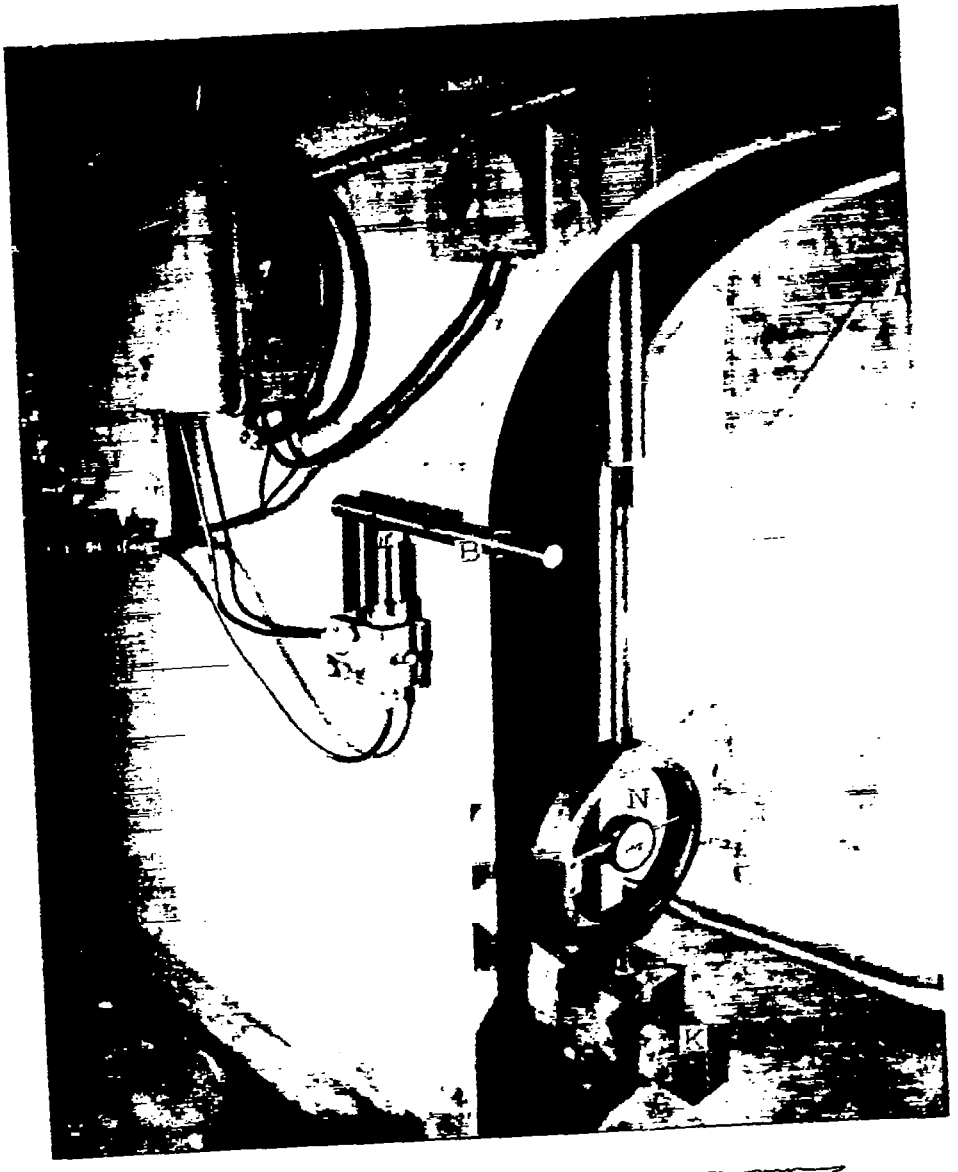

Figure 9.- Measurement of fluctuating axial load.

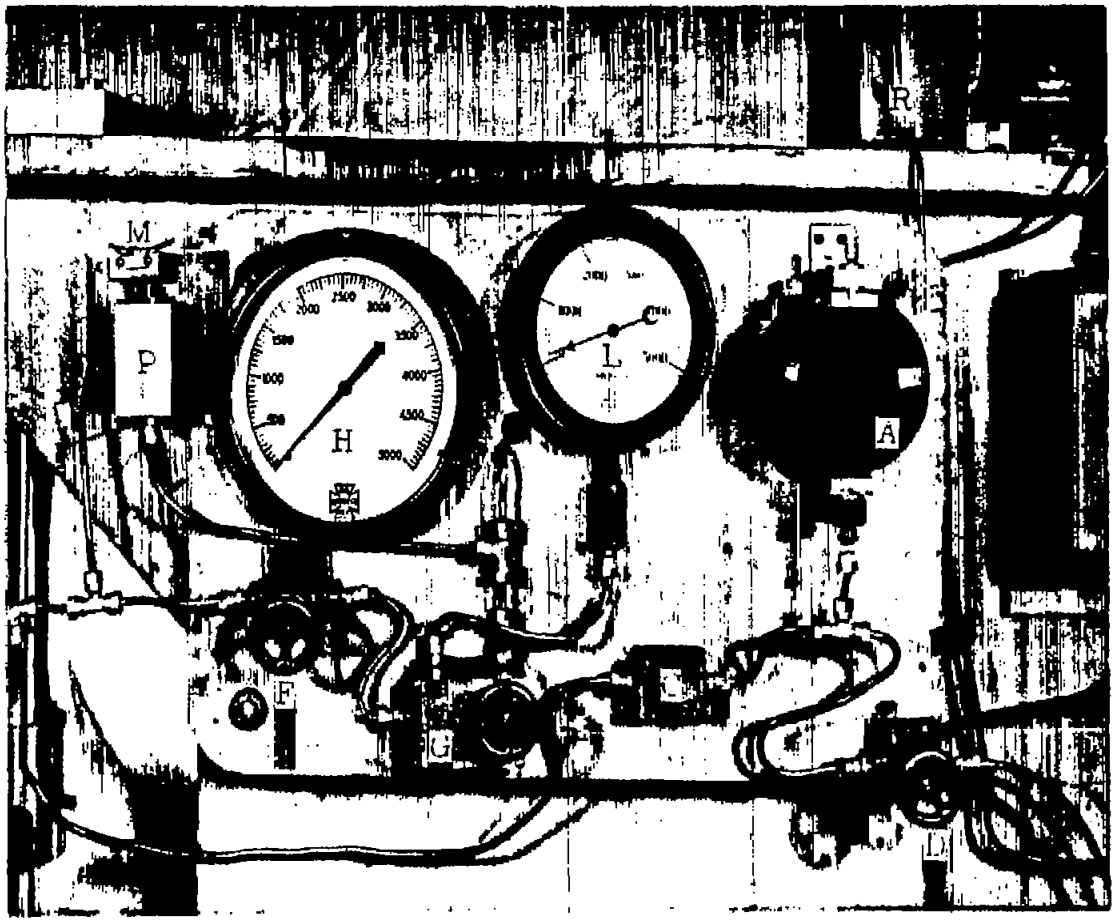

Figure 10.- Panel for measurement of pressures.

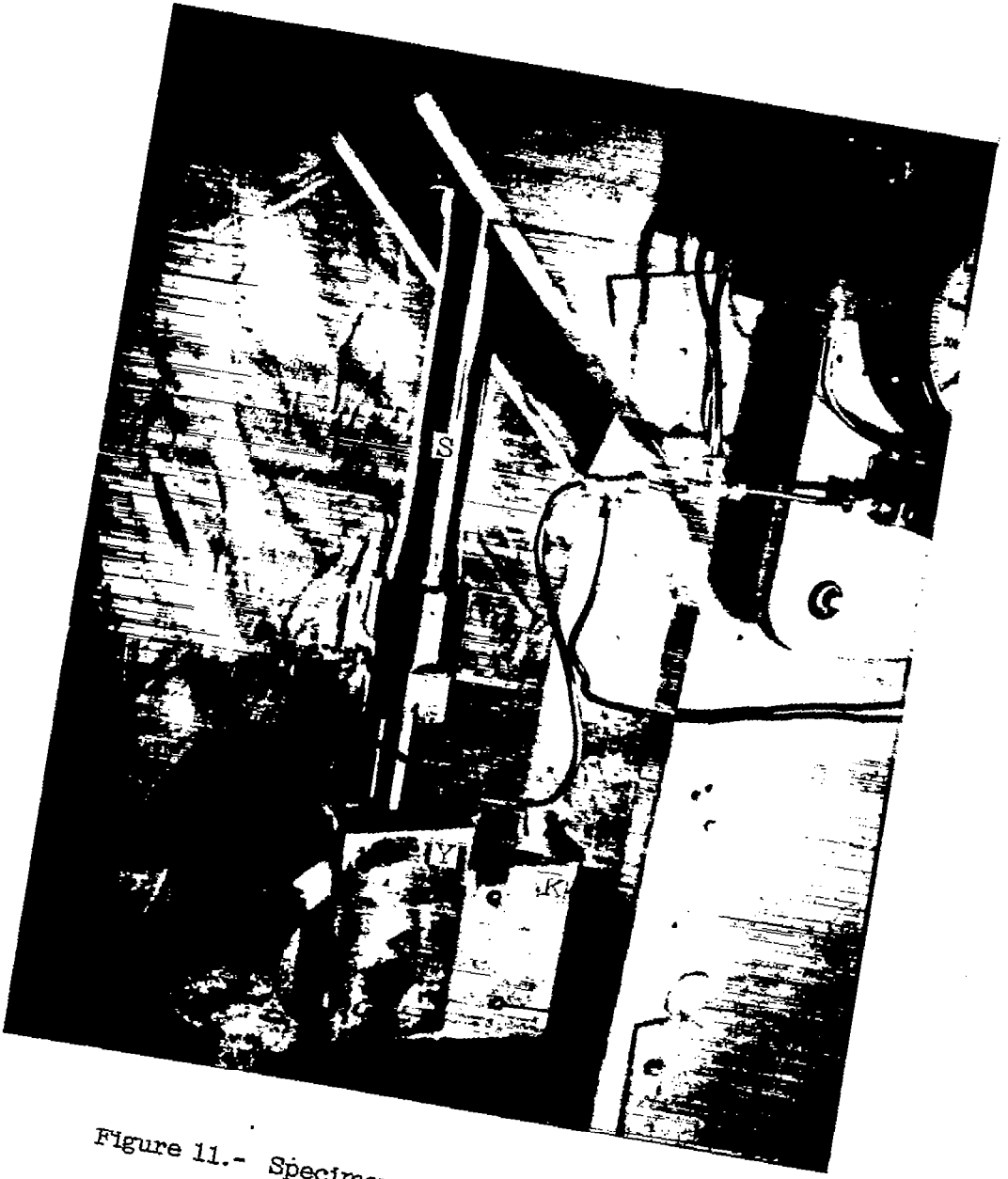

Figure 11.- Specimen in position for testing.

NACA

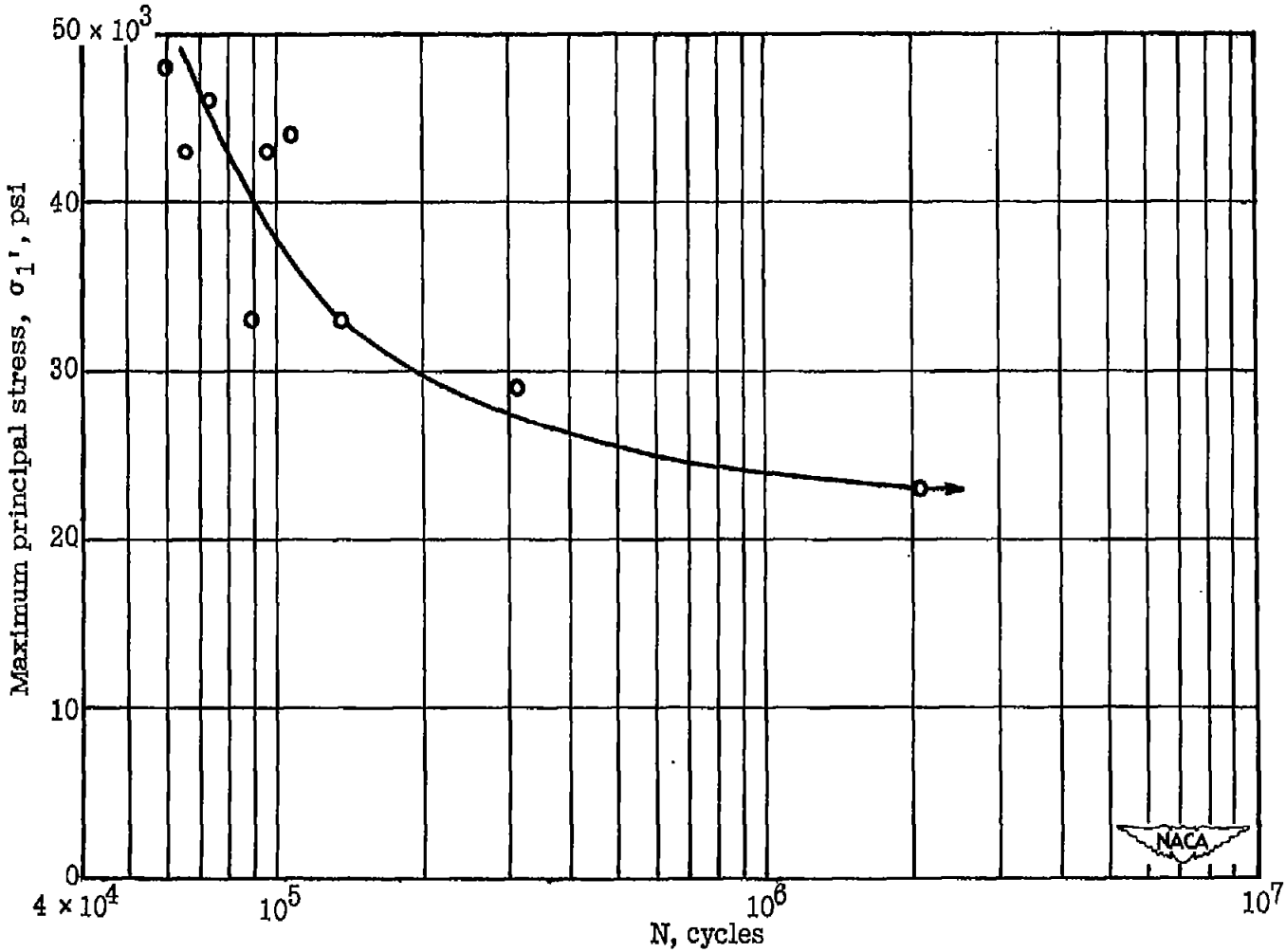

(a) For stress ratio $R = \sigma_2'/\sigma_1' = 0$.

Figure 12.- S-N curves.

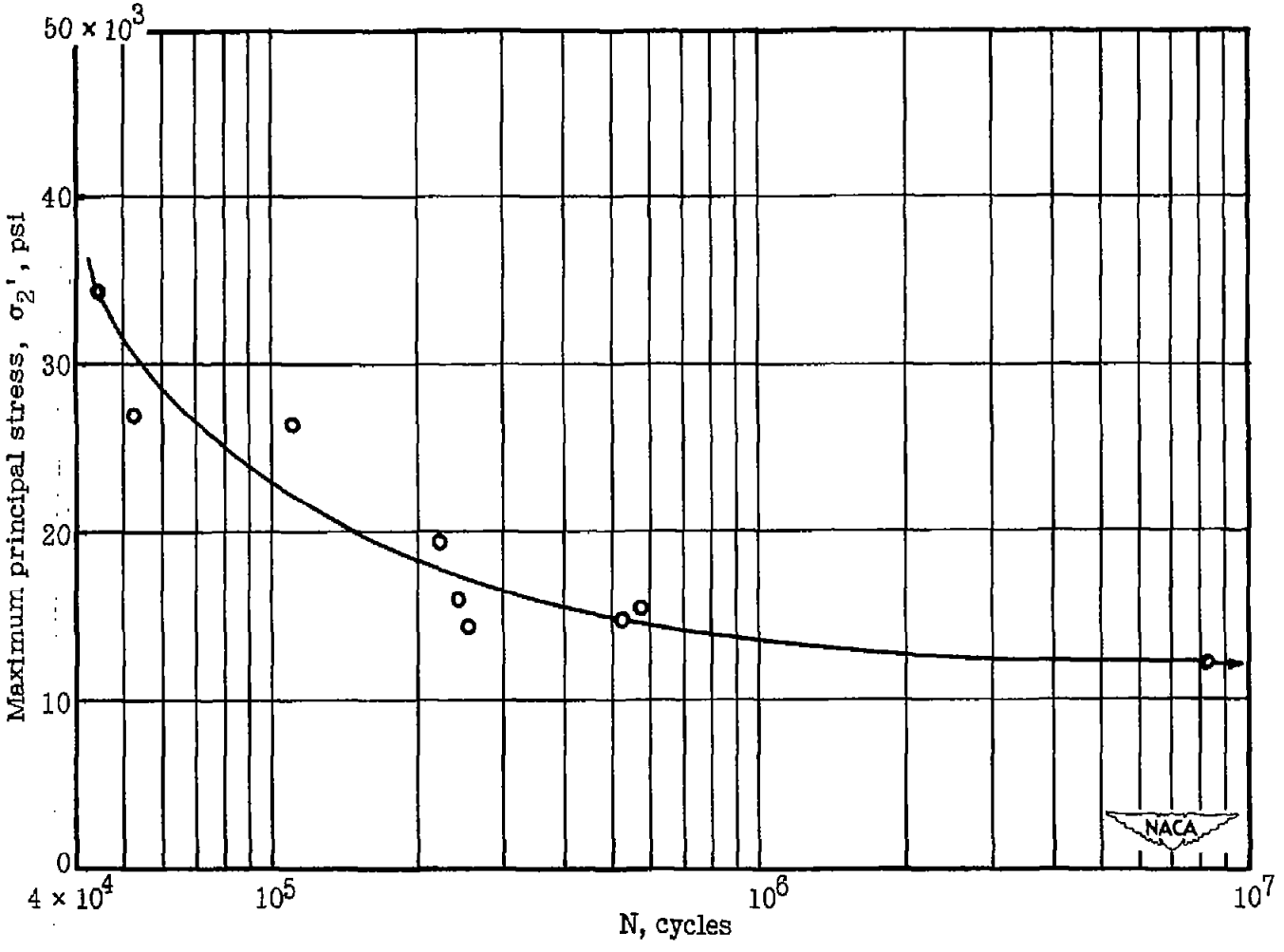

(b) For stress ratio $R = \sigma_2'/\sigma_1' = 2$.

Figure 12.- Continued.

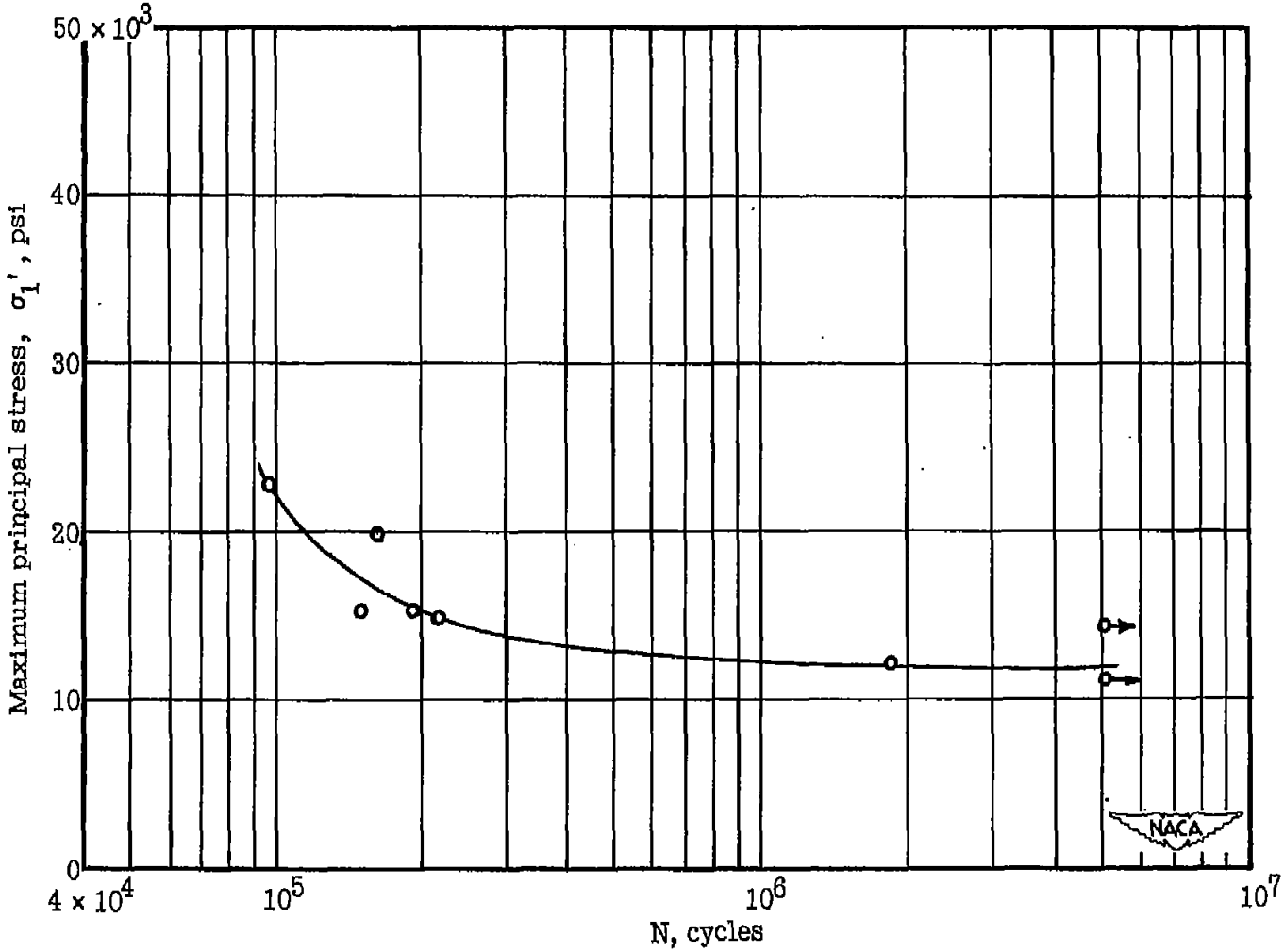

(c) For stress ratio $R = \sigma_2'/\sigma_1' = 1$.

Figure 12.- Continued.

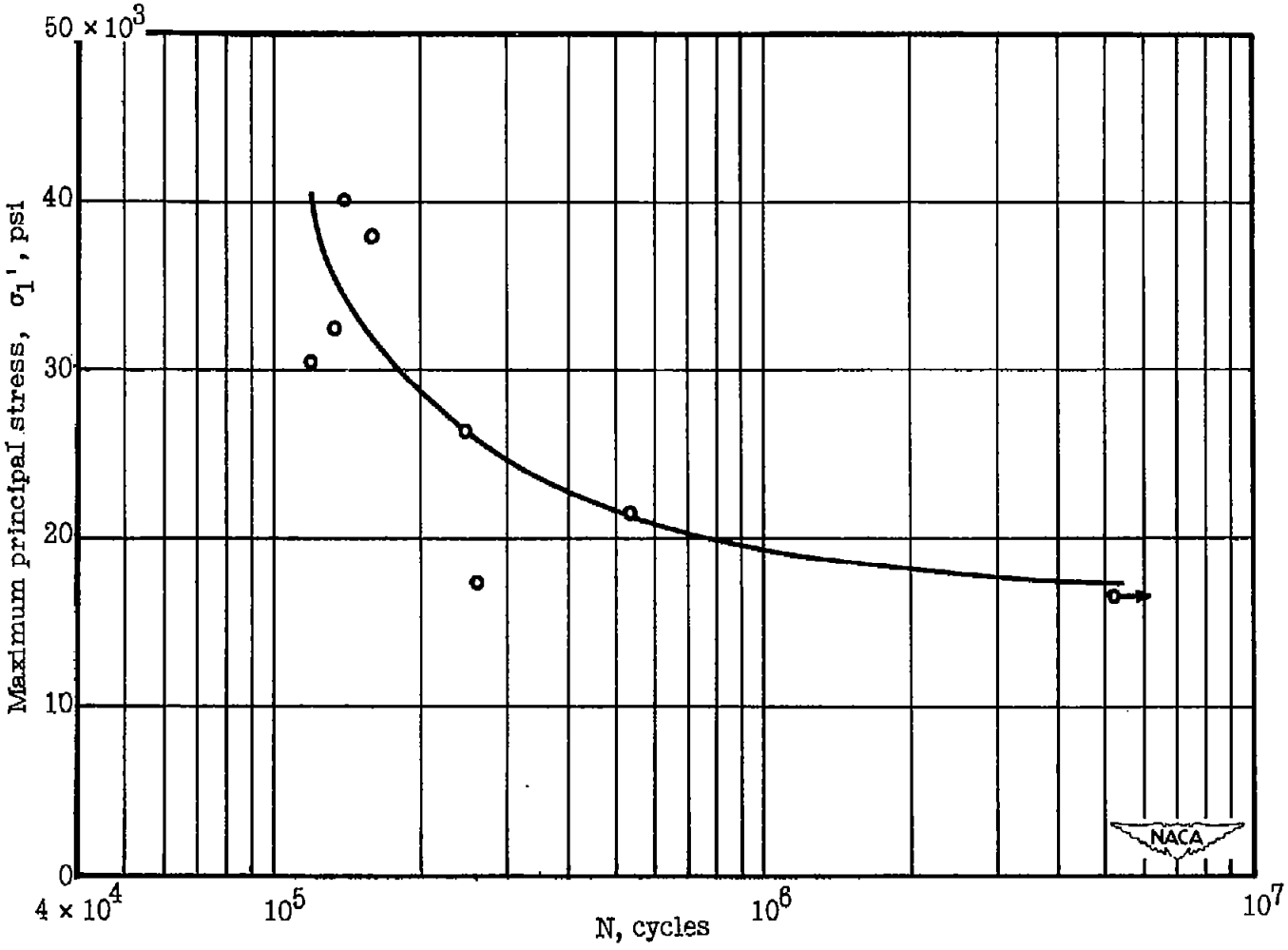

(d) For stress ratio $R = \sigma_2'/\sigma_1' = 0.5$.

Figure 12.- Concluded.

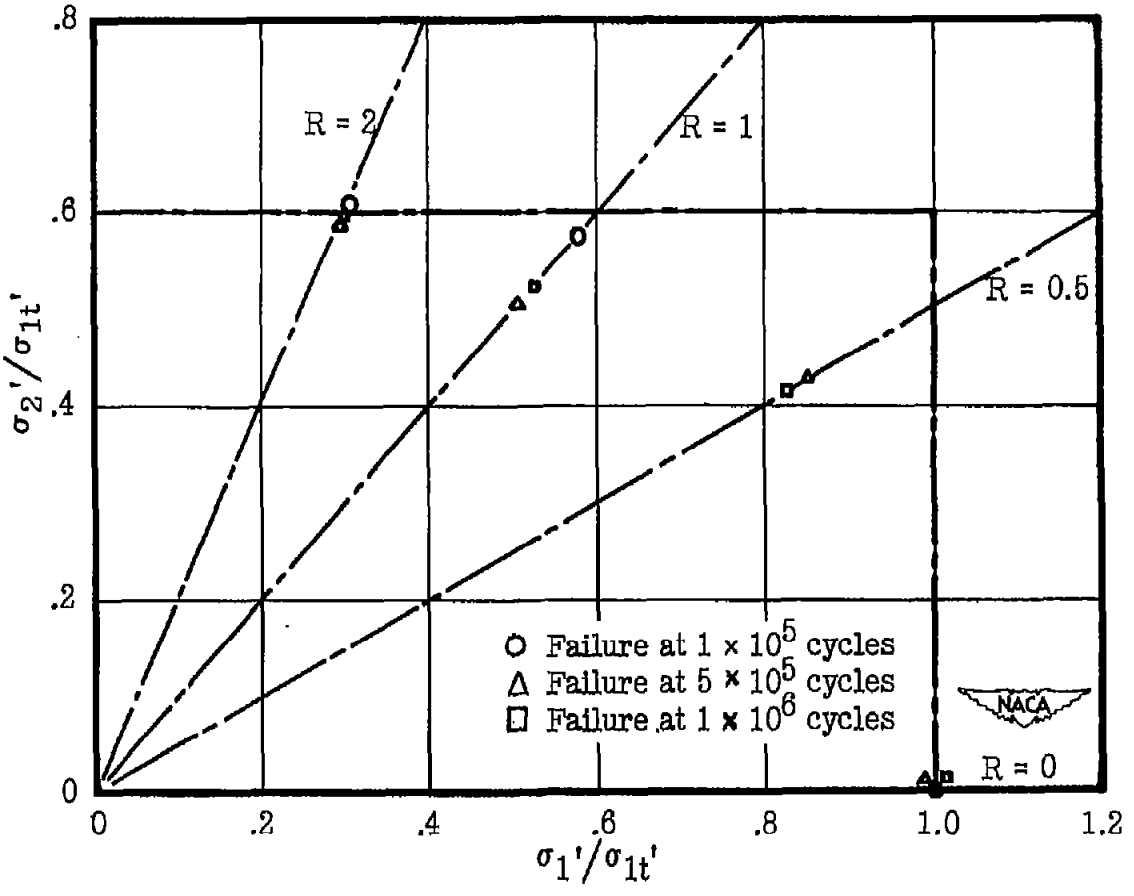

Figure 13.- Biaxial fatigue-stress relationship. 24S-T extruded aluminum-alloy tubing.

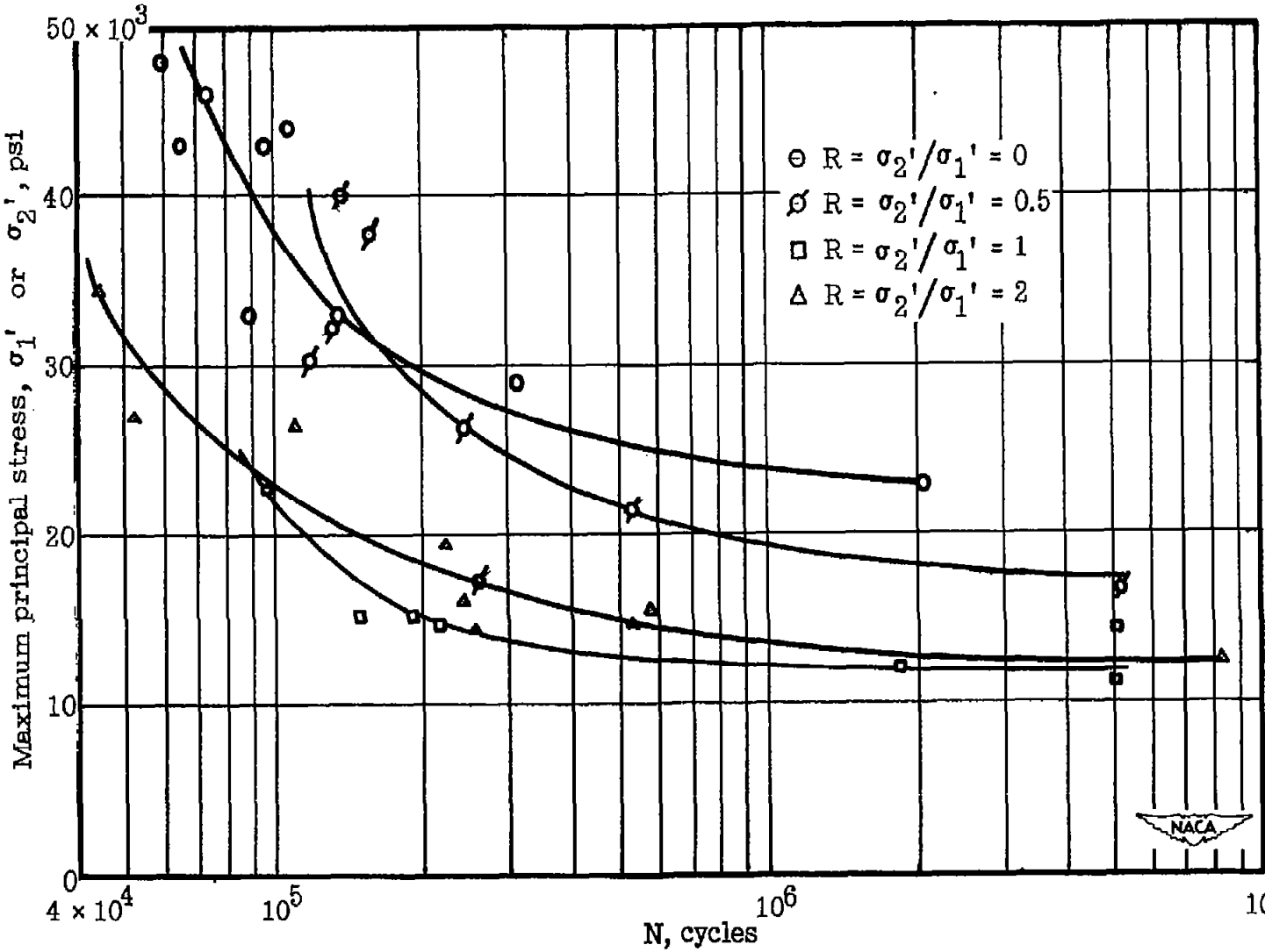

Figure 14.- S-N curves of figure 12 shown in a single plot. 24S-T aluminum-alloy tubing.

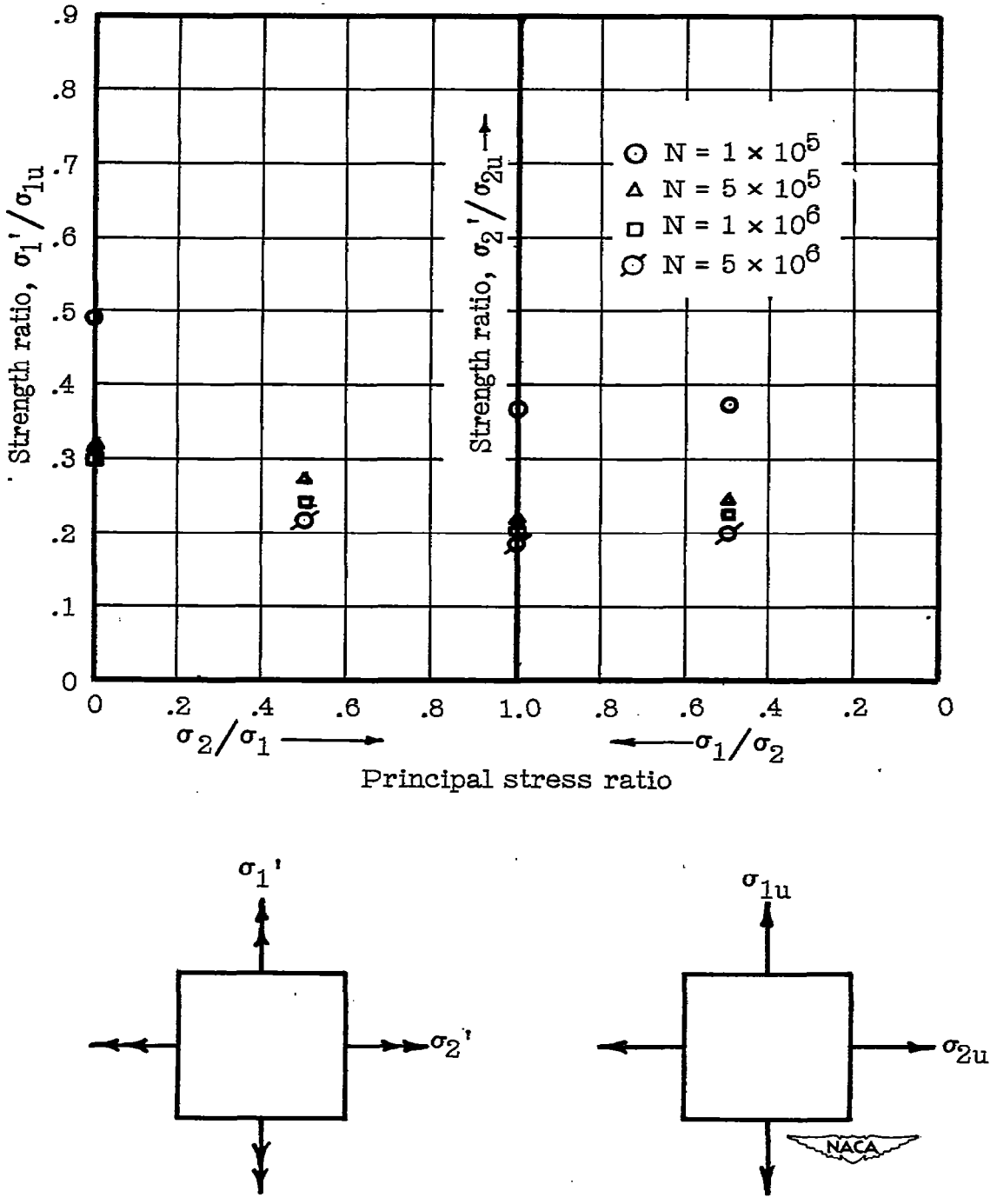

Figure 15.- Comparison of biaxial fatigue and biaxial ultimate strengths.

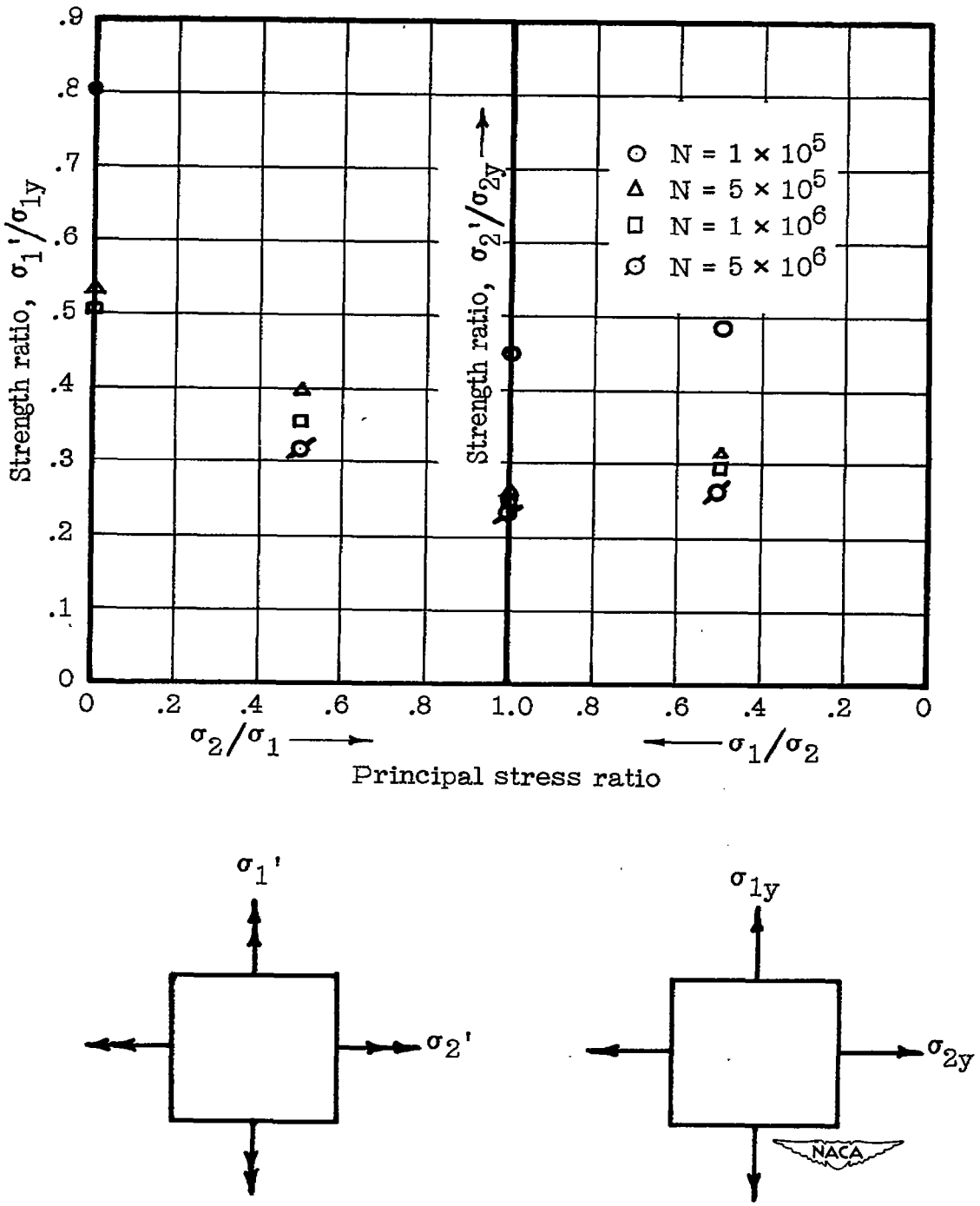

Figure 16.- Comparison of biaxial fatigue and biaxial yield strengths.

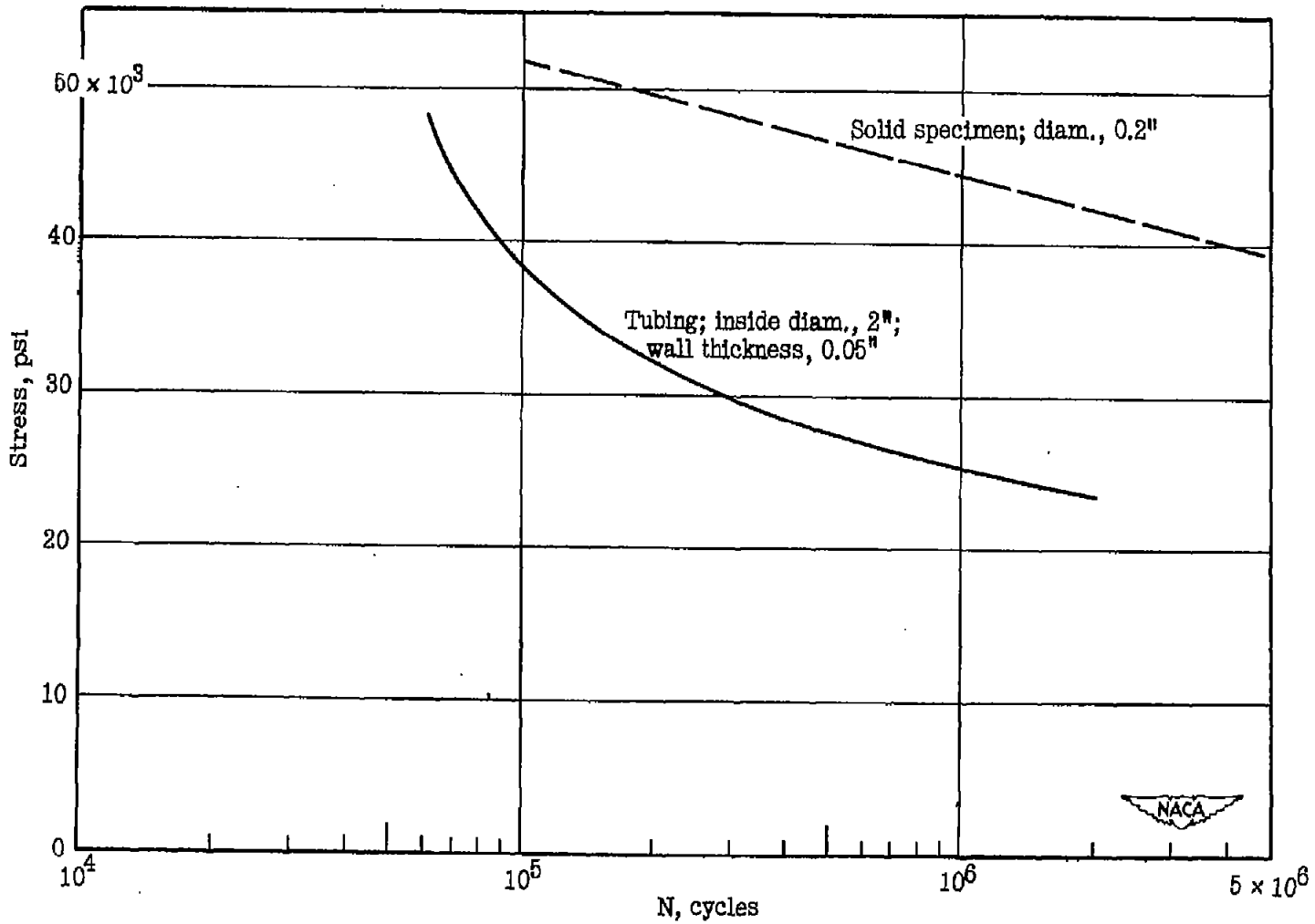

Figure 17.- Comparison between S-N diagram based on present longitudinal fatigue-stress results and S-N diagram based on data given in reference 3 for 0.2-inch-diameter specimens.

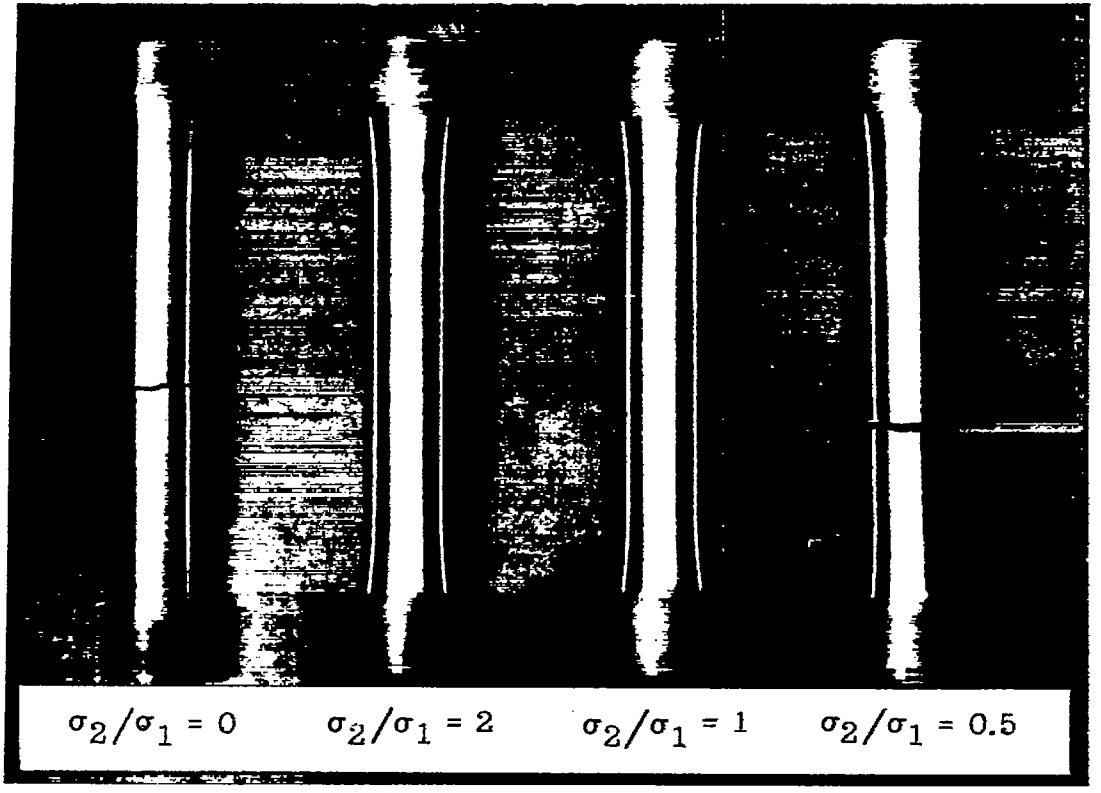

Figure 18.- Typical fractured specimens.